euspen's 22nd International Conference & Exhibition, Geneva, CH, May/June 2022
www.euspen.eu

Rapid evaluation for dynamics of machine tools based on improved reduced order models

Yiwei Ma[1], Yanling Tian[1], Xianping Liu[1]

[1] *School of Engineering, The University of Warwick, Coventry CV4 7AL, UK*

Yi-Wei.Ma@warwick.ac.uk

Abstract

This paper presents an effective semi-analytical approach for predicting lower-order dynamics of horizontal machine tools, which is composed of cutting tool kinematics chain, workpiece kinematics chain plus machine bed. First, the governing equations of motion of component substructures within the kinematics chains are formulated by finite element analysis (FEA). Then, the degrees of freedom (DOFs) of internal and external nodes are reduced using dynamic condensation and rigid multipoint constraint, respectively. This is followed by exploiting a general stiffness model of joint substructures connecting component substructures by taking interface stiffness into consideration. Finally, by merging the component and joint substructures, the reduced dynamic model of the entire system is developed based on substructural synthesis. The comparative study shows that the computational results estimated by the proposed approach have very good agreement with those obtained by a full order FE model, including lower-order natural frequencies, mode shapes of the entire system, and frequency response functions (FRF) between the tool and workpiece. The merits of this approach lie in that the established model enables the full set of lower-order dynamics of the entire system within the workspace to be predicted in a computationally effective and accurate manner.

Keywords: Machine tools, Dynamic modelling, Modal reduction, Interface reduction, Rigid multipoint constraint

1. Introduction

Dynamic behaviour is one of the most important performance factors of machine tools since they are mainly designed and developed for machining where the spindle is excited by dynamic loadings caused by tool-workpiece interaction. Finite element analysis (FEA) is the most accurate method since the 3-dimension geometry of components, contact elasticity of joints can be precisely meshed and modelled [1]. However, the full FE model has to be re-meshed over and over again at different positions of the machine tool, which is pretty time-consuming. Considering dynamic behaviour is highly pose-dependent within the workspace, it is of great importance to establish the dynamic model which can accurately and efficiently evaluate the lower-order natural frequency and FRF (Frequency Response Function) distribution in the whole workspace of the machine tool system in the conceptual design, optimization analysis, and structural modification stage.

To improve the computational efficiency for dynamic behaviour prediction at the stage of conceptual design, the semi-analytical model is proposed based on different techniques. The component mode synthesis is mostly used in the modelling of machine tools where each substructure is modelled by a set of interface DOFs complemented by a set of modal DOFs corresponding to the interior DOFs based on the FE model [2,3]. However, the CMS mainly focuses on the DOFs of internal nodes, instead of the interface nodes, which still contain a large number of DOFs and influence the computational efficiency. The interface nodes can be reduced or expressed efficiently based on the rigid multipoint constraint and interpolation multipoint constraint [4].

By merging the dynamic condensation and rigid multipoint constraint organically, this paper presents a general approach for the rapid evaluation of machine tools' dynamics. The major interests will be focused on the establishment of a model for components based on the substructure and interface reduction. The paper is organized as follows: Having addressed a brief introduction to the dynamic modelling methodology in Section 1, a generalized method for dynamic modelling of kinematics chains is presented in Section 2, including reduction model of component substructure, stiffness model of joint substructure, and substructure synthesis. Then, by taking a horizontal machine tool named M800H as an example, a comparative study is calculated and compared with the results obtained by the full FE model in Section 3 to illustrate the effectiveness of the proposed semi-analytical approach, before conclusions are summarized in Section 4.

2. Generalized dynamic model for kinematics chain

Figure 1 shows the schematic diagram of the kinematics chain comprising several components by mechanical joints, which can be seen as the simplified model of cutting-tool or

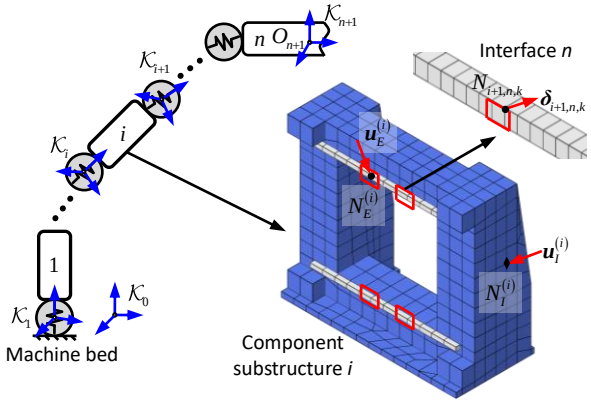

Fig.1 Schematic of general kinematic chain

workpiece chain of the machine tool.

2.1 Reduction model of component substructure

Without loss of generality, consider the component substructure i in the kinematics chain. Regardless of the number of the component substructure, the undamped equation of motion can be represented in its body-fixed frame:

$$\boldsymbol{m}\ddot{\boldsymbol{u}}+\boldsymbol{k}\boldsymbol{u}=\boldsymbol{f} \tag{1}$$

where $\boldsymbol{m}$ and $\boldsymbol{k}$ are the mass and stiffness matrices, $\boldsymbol{u}$ and $\boldsymbol{f}$ are the nodal displacement and force vector of the full FE model of the component substructure, respectively. To derive the reduced model, partition u into two subsets, i.e. the exterior nodal displacement vector $\boldsymbol{u}_E$ and the interior nodal displacement vector $\boldsymbol{u}_I$ as shown in Fig. 1 such that

$$\boldsymbol{u}=\begin{pmatrix}\boldsymbol{u}_E\\ \boldsymbol{u}_I\end{pmatrix},\ \boldsymbol{m}=\begin{bmatrix}\boldsymbol{m}_{EE} & \boldsymbol{m}_{EI}\\ \boldsymbol{m}_{IE} & \boldsymbol{m}_{II}\end{bmatrix},\ \boldsymbol{k}=\begin{bmatrix}\boldsymbol{k}_{EE} & \boldsymbol{k}_{EI}\\ \boldsymbol{k}_{IE} & \boldsymbol{k}_{II}\end{bmatrix},\ \boldsymbol{f}=\begin{pmatrix}\boldsymbol{f}_E\\ \boldsymbol{f}_I\end{pmatrix} \tag{2}$$

The exterior nodal displacement vector $\boldsymbol{u}_E$ can be further expressed according to the joints such that

$$\boldsymbol{u}_E=\begin{pmatrix}\boldsymbol{u}_i\\ \boldsymbol{u}_{i+1}\end{pmatrix},\ \boldsymbol{u}_{i+1}=\begin{pmatrix}\boldsymbol{u}_{i+1,1}\\ \vdots\\ \boldsymbol{u}_{i+1,N}\end{pmatrix},\ \boldsymbol{u}_{i+1,n}=\begin{pmatrix}\boldsymbol{\delta}_{i+1,n,1}\\ \vdots\\ \boldsymbol{\delta}_{i+1,n,K}\end{pmatrix} \tag{3}$$

where $\boldsymbol{\delta}_{i+1,n,k}$ represents the nodal displacement vector of the kth node in interface n of joint $i+1$.

2.1.1 Reduction of internal nodes

In the modal order reduction, it is assumed that $\boldsymbol{u}$ can be linearly expressed in terms of a reduced nodal displacement vector $\bar{\boldsymbol{u}}$

$$\boldsymbol{u}=\boldsymbol{\Phi}_D\bar{\boldsymbol{u}} \tag{4}$$

$$\bar{\boldsymbol{u}}=\begin{pmatrix}\bar{\boldsymbol{u}}_E\\ \bar{\boldsymbol{u}}_P\end{pmatrix},\ \boldsymbol{\Phi}_D=\begin{bmatrix}\boldsymbol{\Phi}_S & \boldsymbol{\Phi}_P\end{bmatrix}=\begin{bmatrix}\mathbf{1}_{m\times m} & \mathbf{0}\\ \boldsymbol{B} & \boldsymbol{\Psi}_P\end{bmatrix} \tag{5}$$

where $\bar{\boldsymbol{u}}_P$ is the modal coordinate vector corresponding the first p elastic modes by locking all DOFs of $\boldsymbol{u}_E$. $\boldsymbol{\Phi}_D$ denotes the transformation matrix from the reduced nodal displacements to the full FE nodal displacements. $\boldsymbol{B}=-\left(\boldsymbol{k}_{II}^{(i)}\right)^{-1}\boldsymbol{k}_{IE}^{(i)}$ is the equivalent static (Guyan) transformation, and $\boldsymbol{\Psi}_P$ is the modal matrix formed by the first p mode shapes of the constrained substructure by solving a generalized eigenvalue problem.

2.1.2 Condensation of external nodes

Based on the rigid multipoint constraint, a condensation node $N_{i+1,n}$ can be created in the centre of interface n, as shown in Fig. 2. In this case, it can be seen that the interface and the condensation node move together as a rigid system, then

$$\boldsymbol{\delta}_{i+1,n,k}=\boldsymbol{\delta}_{i+1,n}+\boldsymbol{r}_{i+1,n,k}\times\boldsymbol{\varepsilon}_{i+1,n} \tag{6}$$

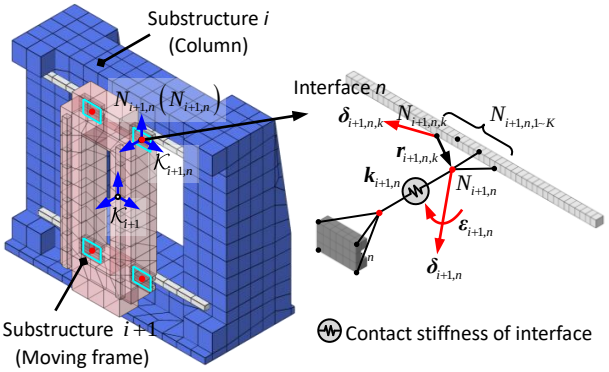

Fig.2 Schematic diagram of interaction between condensation nodes in interface

where $\boldsymbol{\delta}_{i+1,n}$, $\boldsymbol{\varepsilon}_{i+1,n}$ are the displacement and orientation of condensation node $N_{i+1,n}$ expressed in the frame of $\mathcal{K}_{i+1,n}$; $\boldsymbol{r}_{i+1,n,k}$ is the position vector from node $N_{i+1,n,k}$ to condensation node $N_{i+1,n}$ evaluated in frame $\mathcal{K}_{i+1,n}$. Then, $\bar{\boldsymbol{u}}_{i+1,n}$ can be expressed as

$$\bar{\boldsymbol{u}}_{i+1,n}=\bar{\boldsymbol{T}}_{i+1,n}\bar{\boldsymbol{U}}_{i+1,n} \tag{7}$$

$$\bar{\boldsymbol{T}}_{i+1,n}=\begin{bmatrix}\mathbf{1}_{3\times3} & \boldsymbol{r}_{i+1,n,1}\times\\ \vdots & \\ \mathbf{1}_{3\times3} & \boldsymbol{r}_{i+1,n,K}\times\end{bmatrix},\ \bar{\boldsymbol{U}}_{i+1,n}=\begin{pmatrix}\boldsymbol{\delta}_{i+1,n}\\ \boldsymbol{\varepsilon}_{i+1,n}\end{pmatrix} \tag{8}$$

where $\bar{\boldsymbol{U}}_{i+1,n}$ is the nodal displacement vector of $N_{i+1,n}$, and $\bar{\boldsymbol{T}}_{i+1,n}$ is the reduction matrix at interface level.

Similarly, the rigid multipoint constraint can be applied for a second time at the joint level. As shown in Fig. 3, a condensation node N_{i+1} is created in the centre of joint $i+1$, which can be used to describe the motion of interfaces.

$$\bar{\boldsymbol{U}}_{i+1,n}=\tilde{\boldsymbol{T}}_{i+1,n}\tilde{\boldsymbol{U}}_{i+1} \tag{9}$$

$$\tilde{\boldsymbol{T}}_{i+1,n}=\begin{bmatrix}\mathbf{1}_{3\times3} & \boldsymbol{r}_{i+1,n}\times\\ \mathbf{0} & \mathbf{1}_{3\times3}\end{bmatrix},\ \tilde{\boldsymbol{U}}_{i+1}=\begin{pmatrix}\boldsymbol{\delta}_{i+1}\\ \boldsymbol{\varepsilon}_{i+1}\end{pmatrix} \tag{10}$$

where $\tilde{\boldsymbol{U}}_{i+1}$ is the nodal displacement vector of N_{i+1}, and $\tilde{\boldsymbol{T}}_{i+1,n}$ is the reduction matrix at joint level. $\boldsymbol{r}_{i+1,n}$ is the position vector from node $N_{i+1,n}$ to condensation node N_{i+1} evaluated

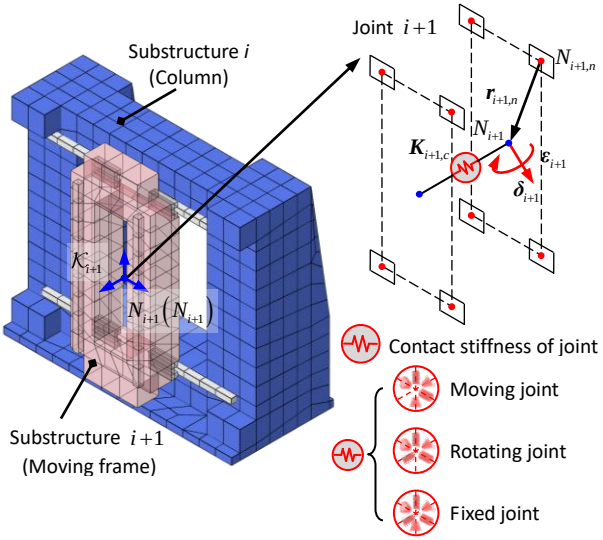

Fig.3 Schematic diagram of interaction between condensation nodes in joint

in the frame $\mathcal{K}_{i+1}$. Substituting Eq. (9) into Eq. (7) leads to

$$\bar{\boldsymbol{u}}_{i+1,n}=\bar{\boldsymbol{T}}_{i+1,n}\tilde{\boldsymbol{T}}_{i+1,n}\tilde{\boldsymbol{U}}_{i+1} \tag{11}$$

Then, $\bar{\boldsymbol{u}}_{i+1}$ can be expressed as

$$\bar{\boldsymbol{u}}_{i+1}=\boldsymbol{T}_{i+1}\tilde{\boldsymbol{U}}_{i+1},\ \boldsymbol{T}_{i+1}=\begin{bmatrix}\bar{\boldsymbol{T}}_{i+1,1}\tilde{\boldsymbol{T}}_{i+1,1} & & \\ & \ddots & \\ & & \bar{\boldsymbol{T}}_{i+1,N}\tilde{\boldsymbol{T}}_{i+1,N}\end{bmatrix} \tag{12}$$

where $\boldsymbol{T}_{i+1}$ is the transformation matrix from the condensation nodal displacements to the FE nodal displacements at joint $i+1$. For joint i

$$\bar{\boldsymbol{u}}_i=\boldsymbol{T}_i\tilde{\boldsymbol{U}}_i \tag{13}$$

Substituting Eq. (12) and Eq. (13) into Eq. (4) leads to

$$\bar{\boldsymbol{u}}=\boldsymbol{T}\tilde{\boldsymbol{U}} \tag{14}$$

$$\boldsymbol{T}=\begin{bmatrix}\boldsymbol{T}_i & & \\ & \boldsymbol{T}_{i+1} & \\ & & \mathbf{1}_{P\times P}\end{bmatrix},\ \tilde{\boldsymbol{U}}=\begin{pmatrix}\tilde{\boldsymbol{U}}_i\\ \tilde{\boldsymbol{U}}_{i+1}\\ \tilde{\boldsymbol{U}}_P\end{pmatrix} \tag{15}$$

Having developed the reduced model of the component substructure evaluated in the body-fixed frame $\mathcal{K}_C$, the following coordinate transformation can be made to map the reduced nodal displacements from its body-fixed frame to the global reference frame $\mathcal{K}$

$$\tilde{\boldsymbol{U}}=\boldsymbol{T}_C\boldsymbol{U} \tag{16}$$

where $\boldsymbol{T}_C=\mathrm{diag}\begin{bmatrix}\boldsymbol{R}_C & \cdots & \boldsymbol{R}_C\end{bmatrix}$ with $\boldsymbol{R}_C$ being the orientation matrix of $\mathcal{K}_C$ with respect to $\mathcal{K}$. Substituting Eq. (16) to Eq. (14), and then to Eq. (4) leads to

$$\boldsymbol{u}=\boldsymbol{\Phi}_D\boldsymbol{T}\boldsymbol{T}_C\boldsymbol{U} \tag{17}$$

such that

$$\boldsymbol{M}\ddot{\boldsymbol{U}}+\boldsymbol{K}\boldsymbol{U}=\boldsymbol{F} \tag{18}$$

$$\boldsymbol{M}=\left(\boldsymbol{\Phi}_D\boldsymbol{T}\boldsymbol{T}_C\right)^{\mathrm{T}}\boldsymbol{m}\left(\boldsymbol{\Phi}_D\boldsymbol{T}\boldsymbol{T}_C\right),\ \boldsymbol{K}=\left(\boldsymbol{\Phi}_D\boldsymbol{T}\boldsymbol{T}_C\right)^{\mathrm{T}}\boldsymbol{k}\left(\boldsymbol{\Phi}_D\boldsymbol{T}\boldsymbol{T}_C\right) \tag{19}$$

where ***M*** and ***K*** are the reduced mass and stiffness matrices, ***U*** and ***F*** are the nodal displacements and nodal force vectors of the component substructure evaluated in $\mathcal{K}$. It is clear that the component substructure can be described by a group of generalized nodes with $(12+P)$DOFs, which can significantly reduce the dimension of calculation.

2.2 Stiffness model of joint substructure

Under rigid multipoint constraint, the relationship between the constraint stiffness of interface and joint can be derived based on the screw theory, as shown in Fig. 4.

$$\boldsymbol{K}_{i+1,c}=\sum_{n=1}^{N}\boldsymbol{X}_{i+1,n}^{-\mathrm{T}}\boldsymbol{k}_{i+1,n}\boldsymbol{X}_{i+1,n}^{-1},\ \boldsymbol{X}_{i+1,n}=\begin{bmatrix}\mathbf{1}_{3\times3} & \mathbf{0}\\ \boldsymbol{r}_{i+1,n}\times & \mathbf{1}_{3\times3}\end{bmatrix} \tag{20}$$

where $\boldsymbol{K}_{i+1,c}$ is the constraint stiffness of joint $i+1$, $\boldsymbol{k}_{i+1,n}$ is the constraint stiffness of interface *n*, and $\boldsymbol{X}_{i+1,n}$ represents the adjoint transformation matrix.

The actuation stiffness of joint $i+1$ with Fixed-Fixed support can be modelled as

$$\frac{1}{k_{i+1,a}}=\frac{1}{\left(\frac{1}{k_{b1}}+\frac{1}{k_{l1}}\right)^{-1}+\left(\frac{1}{k_{b2}}+\frac{1}{k_{l2}}\right)^{-1}}+\frac{1}{k_{nut}} \tag{21}$$

where k_{nut} is the stiffness of nut, k_{b1} and k_{b2} are stiffness of the front and rear bearing, respectively, and $k_{l1}^{-1}=l_1/EA$, $k_{l2}^{-1}=l_2/EA$ (as shown in Fig. 5). Then the 6-DOFs stiffness matrix of the joint can be written as

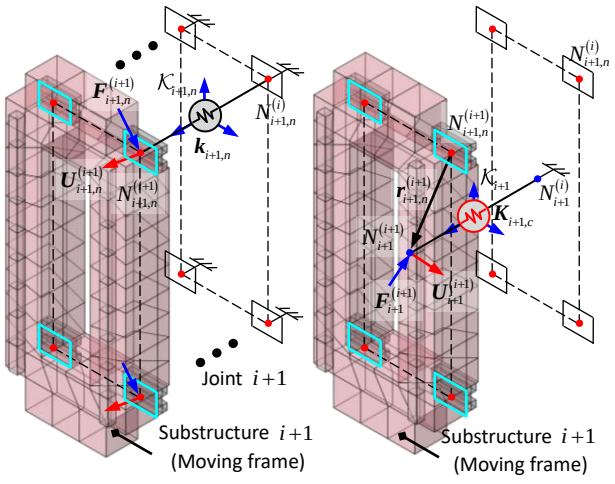

(a) Constraint stiffness of interface (b) Constraint stiffness of joint

Fig.4 The relationship between interface stiffness and joint stiffness

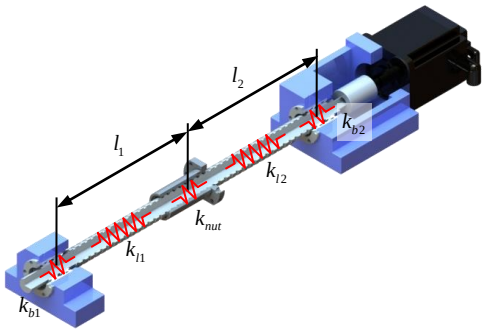

Fig.5 Actuation stiffness of the feed drive system

$$\boldsymbol{K}_{J,i+1}=\begin{bmatrix}k_{i+1,a} & \mathbf{0}\\ \mathbf{0} & \boldsymbol{K}_{i+1,c}\end{bmatrix} \tag{22}$$

2.3 Substructure synthesis

Regardless of the kinetic energy of the joint substructure, the total kinetic energy and potential energy of the entire machine tool can be derived as

$$T=\sum_{i=1}^{n}T_{S,i},\ V=\sum_{i=1}^{n}V_{S,i}+\sum_{i=1}^{n}V_{J,i} \tag{23}$$

$$T_{S,i}=\frac{1}{2}\left(\dot{\boldsymbol{U}}^{(i)}\right)^{\mathrm{T}}\boldsymbol{M}^{(i)}\dot{\boldsymbol{U}}^{(i)},\ V_{S,i}=\frac{1}{2}\left(\boldsymbol{U}^{(i)}\right)^{\mathrm{T}}\boldsymbol{K}^{(i)}\boldsymbol{U}^{(i)} \tag{24}$$

$$V_{J,i}=\frac{1}{2}\begin{pmatrix}\boldsymbol{U}_2^{(i)}\\ \boldsymbol{U}_1^{(i+1)}\end{pmatrix}^{\mathrm{T}}\begin{bmatrix}\boldsymbol{K}_{J,i} & -\boldsymbol{K}_{J,i}\\ -\boldsymbol{K}_{J,i} & \boldsymbol{K}_{J,i}\end{bmatrix}\begin{pmatrix}\boldsymbol{U}_2^{(i)}\\ \boldsymbol{U}_1^{(i+1)}\end{pmatrix},\ \boldsymbol{U}^{(i)}=\begin{pmatrix}\boldsymbol{U}_1^{(i)}\\ \boldsymbol{U}_2^{(i)}\\ \boldsymbol{U}_P^{(i)}\end{pmatrix} \tag{25}$$

where $T_{S,i}$ and $V_{S,i}$ represent the kinetic energy and potential energy of component substructure *i*, and $V_{J,i}$ is the potential energy of joint substructure *i*. From Eq. (23), the undamped equation of motion can be assembled in the frame $\mathcal{K}$.

$$\boldsymbol{M}\ddot{\boldsymbol{U}}+\boldsymbol{K}\boldsymbol{U}=\boldsymbol{F} \tag{26}$$

where ***M*** is a block diagonal matrix, and ***K*** is a banded matrix.

3. Numerical example

In this section, the dynamic model of a 4-axis 'box-in-box' horizontal machine tool, named M800H as shown in Fig.6, is established to illustrate the accuracy and effectiveness of the proposed method. The workspace of the machine tool is defined as a cube with the length of one side 800mm, which means the coordinates of the *X*/*Y*/*Z* axis are all from $-400\mathrm{mm}\sim+400\mathrm{mm}$. The reference configuration is defined as $(0\ \ 0\ \ 0)\mathrm{mm}$.

Fig. 7 shows the first six mode shapes of the machine tool predicted by the proposed model and an FE model established by using commercial software SAMCEF at the reference

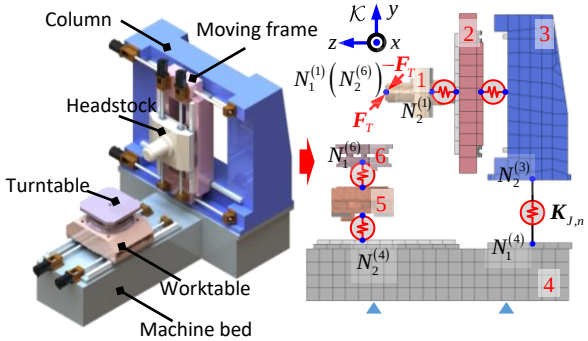

Fig.6 Overview of machine tool with 'box-in-box' type

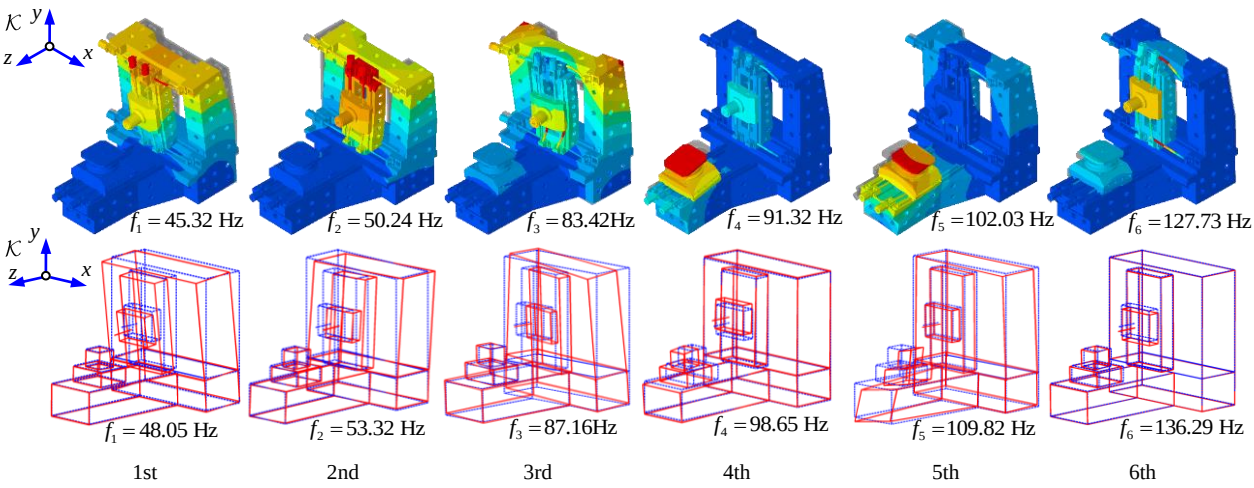

Fig 7. Mode shapes of the M800H machine tool obtained by SAMCEF and the semi-analytical approach

configuration. The results show that the mode shapes predicted by the FE model match well with those obtained by the proposed model. Then, the Modal Assurance Criterion (MAC) is employed to verify the consistency between mode shapes by two models. Fig. 8 shows clearly that the values of diagonal elements are much larger than those of the non-diagonal elements, confirming the validity of the proposed model for predicting the lower-order dynamics of the machine tool. In addition, the maximum discrepancy of the natural frequencies calculated between the two models is less than 7%, which demonstrates the accuracy of the proposed model. Fig. 9 shows FRFs between tool and workpiece along the x, y, and z axes of $\mathcal{K}$. The damping ratio for all modes is set to be 0.03 identically in the two models. Clearly, the results calculated by the proposed model are a little higher than the FE model since the rigid multipoint constraints improve the potential energy of the joint substructure. Fig. 10 shows the distributions of the first fourth natural frequencies across the entire workpiece, which were obtained with no more than 1 second using a laptop equipped with an Intel i7-8750 CPU and 16 GB RAM.

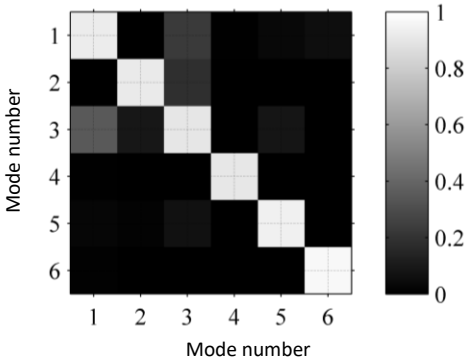

Fig.8 MAC of the first sixth mode shaped between the semi-analytical model and the FE model

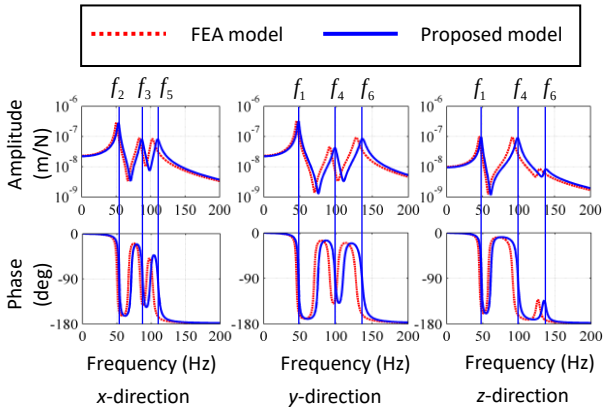

Fig.9 The FRFs at the reference configuration

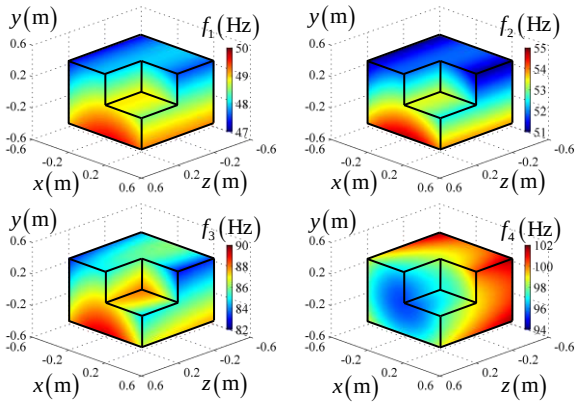

Fig.10 Natural frequencies distributions across the entire workpiece

4. Conclusions

This paper presents a rapid and effective approach to predict the dynamic performances of the machine tool. The conclusions are drawn as follows

(1) By combining FEA with modal reduction and interface reduction technique, the reduced model of component substructure is proposed. Then, the stiffness model of joint substructure is derived by screw theory. Finally, merging the elastic potential and kinetic energies of the entire system results in the general dynamic model of kinematics chains.

(2) A comparison study between FEA and the proposed model is developed to demonstrate the effectiveness of the proposed model. The results show that the dynamic performances can be predicted with sufficient computational accuracy and huge computational time savings across the entire workspace.

References

[1] Nam, H. H., & Altintas, Y. (2020). Modeling the dynamics of 5-axis machine tool using the multibody approach. Journal of Manufacturing Science and Engineering, 143(2), 021012.

[2] Law, M., Phani, A. S., & Altintas, Y. (2013). Position-dependent multibody dynamic modeling of machine tools based on improved reduced order models. Journal of Manufacturing Science & Engineering, 135(2), 2186-2199.

[3] Law, M., Altintas, Y., & Phani, A.S. (2013). Rapid evaluation and optimization of machine tools with position-dependent stability. International Journal of Machine Tools & Manufacture, 68, 81-90.

[4] Heirman, G., & Desmet, W. (2010). Interface reduction of flexible bodies for efficient modeling of body flexibility in multibody dynamics. Multibody System Dynamics, 24(2), 219-234.